Journal of Molecular Catalysis A: Chemical 296 (2008) 9–17

Contents lists available at ScienceDirect

Journal of Molecular Catalysis A: Chemical

journal homepage: www.elsevier.com/locate/molcata

Synthesis, structure, and catalytic ethylene oligomerization of nickel complexes bearing 2-pyrazolyl substituted 1,10-phenanthroline ligands

Yue Yang[a,c], Peiju Yang[a], Cui Zhang[a,c], Gang Li[a], Xiao-Juan Yang[a], Biao Wu[a,*], Christoph Janiak[b,*]

[a] State Key Laboratory for Oxo Synthesis & Selective Oxidation, Lanzhou Institute of Chemical Physics, Chinese Academy of Sciences, Lanzhou 730000, China
[b] Institut für Anorganische und Analytische Chemie, Universität Freiburg, Albertstr. 21, D-79104 Freiburg, Germany
[c] Graduate School of Chinese Academy of Sciences, Beijing 100049, China

ARTICLE INFO

Article history:
Received 17 June 2008
Received in revised form 22 August 2008
Accepted 22 August 2008
Available online 5 September 2008

Keywords:
Nickel complexes
Ethylene oligomerization
Phenanthroline ligand
Nitrogen ligands
Methylalumoxane

ABSTRACT

A series of nickel(II) halide complexes [$NiCl_2$(L)] (**1a–12a**) and [$NiBr_2$(L)] (**1b–12b**) bearing 2-pyrazolyl substituted 1,10-phenanthroline derivatives (**L^1–L^{12}**) have been synthesized and characterized by elemental analysis, IR spectroscopy and X-ray diffraction analysis (for **1a′**, **10b** and **12b**). Upon activation with methylaluminoxane (MAO), these complexes display good catalytic activities in ethylene oligomerization (up to 3.01×10^5 g mol(Ni)$^{-1}$ h^{-1} at 10 atm of ethylene for **12a** with **L^{12}** = 2-(3,5-*diphenyl*pyrazol-1-yl)-9-*mesityl*-1,10-phenanthroline). Complexes with bulkier aryl groups in the 9-position of the phenanthroline ring and the 3- and 5-position of the pyrazolyl ring give higher activities. This is explained with the formation of a more directional environment, a reaction channel around the nickel center which enhances the probability of insertion over dissociation after ethylene coordination to Ni. Also, bulkier aryl substituents can suppress chain-transfer reactions (typically β-H elimination) and therefore increase the activity.

1. Introduction

The oligomerization of ethylene is an important process that is used to convert this basic feedstock into various useful products. The development of new molecular catalysts for the oligomerization and polymerization of ethylene is the key in this area [1,2]. Late transition metal complexes have attracted intense attention in the past decade because of their high activity for ethylene activation, and various catalyst systems have been studied and reviewed [2,3]. Nickel complexes are of great interest in this respect due to their activities in the SHOP process of ethylene oligomerization [4]. A number of nickel complexes have been reported for olefin oligomerization, including tetra-coordinated catalyst precursors containing bidentate ligands such as PˆP [5], PˆO [6], PˆN [7], NˆN [8], and NˆO [9], or penta-coordinated systems with tridentate ligands of NˆNˆO [10], NˆOˆN [11], NˆNˆN [10-13], PˆNˆN [14] and NˆSˆN type [15].

Recently we have been interested in nickel complexes with tridentate NˆNˆN ligands for ethylene oligomerization. For this purpose a series of pyrazolyl-substituted 1,10-phenanthroline compounds have been designed. 1,10-Phenanthroline and its derivatives are widely used as ligands for late transition metal complexes because it is convenient to tailor their steric and electronic structure by varying the substituents [16]. However, late transition metal complexes of 1,10-phenanthrolines have rarely been studied for catalytic ethylene oligomerization/polymerization [17]. We have previously reported the catalytic behavior of some nickel and cobalt complexes with bidentate 2,9-diaryl-1,10-phenanthrolines (NˆN) [18]. Some nickel catalysts with tridentate 2-imino-1,10-phenanthrolines have also been reported recently [19,20]. In the present work, we have explored a series of tridentate (NˆNˆN) 1,10-phenanthrolines bearing 2-pyrazolyl and 9-aryl substituents, and present herein the synthesis and crystal structure of the nickel(II) complexes as well as their catalytic activities for ethylene oligomerization with the assistance of methylaluminoxane (MAO).

2. Results and discussion

2.1. Synthesis

The 2-(3-R^2-5-R^3-pyrazol-1-yl)-9-R^1-1,10-phenanthroline ligands (**L^1–L^{12}**) were synthesized using modified literature procedures, as reported for **L^1** [21] by the Knorr-type cyclization from various diketones (acetylacetone, benzoylacetone or dibenzoylmethane) and 2-hydrazine-9-aryl-1,10-phenanthrolines, as depicted in Scheme 1. Notably, the reaction showed high regioselectivity and only the 3-methyl-5-phenylpyrazolyl isomers have been obtained in the condensation of the asymmetric benzoylacetone

* Corresponding authors. Fax: +86 931 4968286 (B. Wu); fax: +49 761 2036147 (C. Janiak).
E-mail addresses: wubiao@lzb.ac.cn (B. Wu), janiak@uni-freiburg.de (C. Janiak).

1381-1169/$ – see front matter © 2008 Elsevier B.V. All rights reserved.
doi:10.1016/j.molcata.2008.08.015

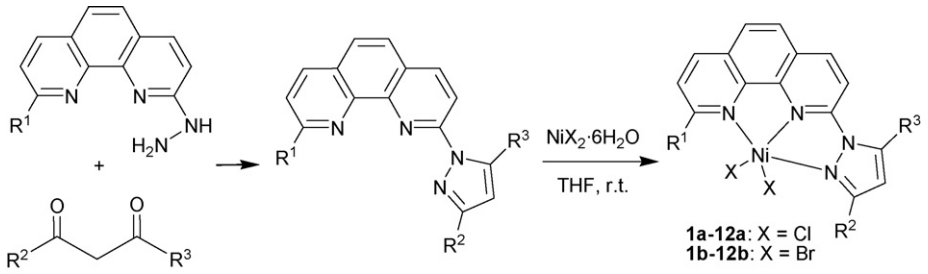

[$NiCl_2$(L)]	1a	2a	3a	4a	5a	6a	7a	8a	9a	10a	11a	12a
[$NiBr_2$(L)]	1b	2b	3b	4b	5b	6b	7b	8b	9b	10b	11b	12b
	L^1	L^2	L^3	L^4	L^5	L^6	L^7	L^8	L^9	L^{10}	L^{11}	L^{12}
R^1	H	H	H	Ph	Ph	Ph	1-Nap	1-Nap	1-Nap	Mes	Mes	Mes
R^2	Me	Me	Ph	Me	Me	Ph	Me	Me	Ph	Me	Me	Ph
R^3	Me	Ph	Ph	Me	Ph	Ph	Me	Ph	Ph	Me	Ph	Ph

Scheme 1. Synthesis of the ligands (L^1–L^{12}) and the complexes [$NiCl_2$(L)] (**1a–12a**) and [$NiBr_2$(L)] (**1b–12b**). 1-Nap = 1-naphthyl, Mes = mesityl (–C_6H_2-2,4,6-Me_3).

with 2-hydrazine-9-aryl-1,10-phenanthrolines (in the cases of ligands L^2, L^5, L^8, and L^{11}), as confirmed by the ^{1}H NMR spectra. The nickel(II) complexes were obtained by treating the THF solution of nickel chloride or bromide salts with the corresponding ligands (L^1–L^{12}) at room temperature in high yields (89–97%, Scheme 1). These complexes are air-stable in both solution and the solid state, and were identified by FT-IR and elemental analysis.

2.2. X-ray crystallographic study

Crystals of the dibromide **10b** and **12b** and the dichloride **1a**′ suitable for single-crystal X-ray diffraction were obtained through slow diffusion of diethyl ether into their dichloromethane (**10b** and **12b**) or methanol (**1a**′) solution. The molecular structures of the complexes are shown in Figs. 1–3, and the selected bond lengths and angles are given in Tables 1 and 2. In general, the complexes [NiX_2(L)] show a 1:1 metal-to-ligand ratio with the metal center being five-coordinated by the tridentate ligand and the halide (X) ligands. The structure of **1a**′ [NiCl(L^1)(H_2O)$_2$]Cl illustrates the effect of excess water during crystallization. The association of aqua ligands changes the nickel coordination polyhedron. In accordance with the tridentate chelating pattern, the central Ni–N2 bond is shorter than the terminal Ni–N1 and Ni–N4 bonds, while the two

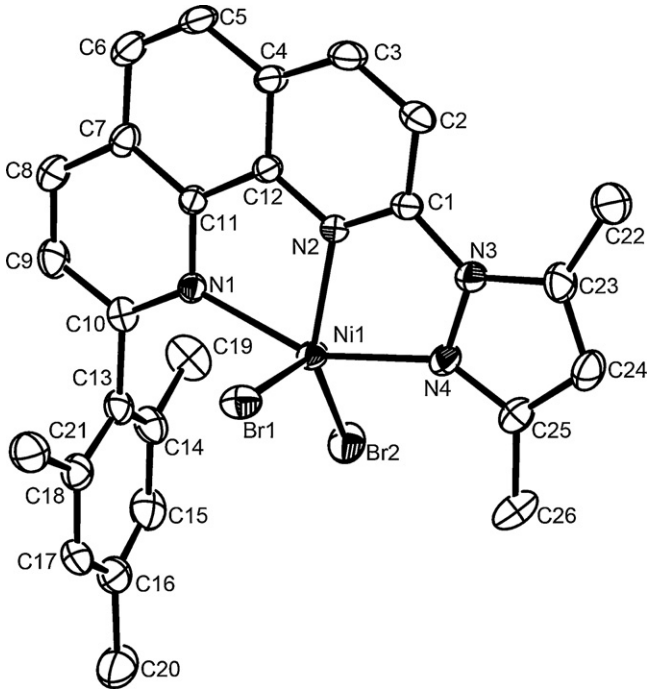

Fig. 1. The molecular structure of **10b** (thermal ellipsoids at the 30% probability level and hydrogen atoms are omitted for clarity).

Table 1
Selected bond lengths (Å) and angles (°) for **10b** and **12b**

10b		**12b**	
Ni1–N1	2.225(3)	Ni1–N1	2.183(3)
Ni1–N2	1.981(3)	Ni1–N2	1.963(4)
Ni1–N4	2.123(4)	Ni1–N4	2.199(4)
Ni1–Br1	2.4506(7)	Ni1–Br1	2.391(1)
Ni1–Br2	2.3541(7)	Ni1–Br2	2.3947(8)
N2–Ni1–N1	78.8(1)	N2–Ni1–N1	79.5(1)
N2–Ni1–N4	76.2(1)	N2–Ni1–N4	76.0(1)
N1–Ni1–N4	154.5(1)	N1–Ni1–N4	155.4(1)
N1–Ni1–Br1	95.21(8)	N1–Ni1–Br1	95.9(1)
N2–Ni1–Br1	94.60(9)	N2–Ni1–Br1	109.0(1)
N4–Ni1–Br1	92.2(1)	N4–Ni1–Br1	93.5(1)
Br2–Ni1–Br1	128.36(3)	Br1–Ni1–Br2	146.17(3)
N1–Ni1–Br2	99.54(9)	N1–Ni1–Br2	96.2(1)
N2–Ni1–Br2	136.7(1)	N2–Ni1–Br2	104.2(1)
N4–Ni1–Br2	94.86(9)	N4–Ni1–Br2	88.4(1)

Table 2
Selected bond lengths (Å) and angles (°) for **1a**′

Ni1–N1	2.138(3)	Ni1–Cl1	2.368(1)
Ni1–N2	1.996(2)	Ni1–O1	2.068(3)
Ni1–N4	2.145(3)	Ni1–O2	2.074(2)
N2–Ni1–N1	79.0(1)	O1–Ni1–O2	84.1(1)
N2–Ni1–N4	75.3(1)	N4–Ni1–Cl1	93.45(8)
N1–Ni1–N4	154.3(1)	O1–Ni1–N1	89.9(1)
N2–Ni1–Cl1	97.08(8)	O1–Ni1–N4	88.1(1)
O2–Ni1–Cl1	90.99(8)	N1–Ni1–Cl1	90.67(9)
N2–Ni1–O2	171.8(1)	O2–Ni1–N1	102.1(1)
N2–Ni1–O1	87.8(1)	O2–Ni1–N4	103.2(1)
O1–Ni1–Cl1	175.08(7)		

bite angles (N1–Ni–N2 and N2–Ni–N4) are comparable to each other in the range 75.3–76.2°.

Complex **10b** displays a distorted square pyramidal geometry around the nickel center (Fig. 1). The three nitrogen donors of the ligand and one of the bromo atoms (Br2) define the basal plane, while the other Br atom (Br1) occupies the apical coordination site. The Ni(II) center is located slightly above the basal plane (0.54 Å). Complex **12b** is also five-coordinated by a ligand and two Br atoms (Fig. 2) [22]. There is a molecule of CH_2Cl_2 in the crystal. While the pyrazole ring is nearly coplanar with the phenanthroline plane in **10b** (dihedral angle 3.4°), it is twisted away in **12b** (17.0°). This could be attributed to the steric effect of the substituents on the pyrazole ring (3,5-dimethyl in **10b** vs 3,5-diphenyl in **12b**). Meanwhile, the Br–Ni–Br angle in **12b** (146.17(3)°) is also significantly widened compared to **10b** (128.36(3)°), and the mesityl group is nearly perpendicular to the phenanthroline plane in **10b** (dihedral angle 88.6°) and **12b** (89.2°) (Table 1).

Complex **1a**′ [NiCl(**L**^{1})$(H_2O)_2$]Cl is obtained from water-containing MeOH/Et_2O. The presence of water changes the coordination mode and sphere of the nickel atom, hence, **1a**′ exhibits a different solid-state structure from the above two complexes. The Ni atom is six-coordinated by a tridentate **L**^{1}, a Cl atom and two aqua ligands with a distorted octahedral geometry (Fig. 3a, Table 2). A second chlorine atom is present as the counter ion. The pyrazole ring is nearly coplanar with the phenanthroline plane (dihedral angle 5.6°), while the two aqua ligands are *cis*-coordinated. The chloro ligand and the chloride anion accept hydrogen bonds from the aqua ligands, leading to a 1D hydrogen-bonded zigzag chain along the *c*-axis (Fig. 3b). It should be noted that attempts to crystallize this compound in the [$NiCl_2$(L)] form have been unsuccessful. However, while the crystals were obtained from methanol/ether, the powder samples used for the catalytic investigation were prepared in THF and were carefully dried to

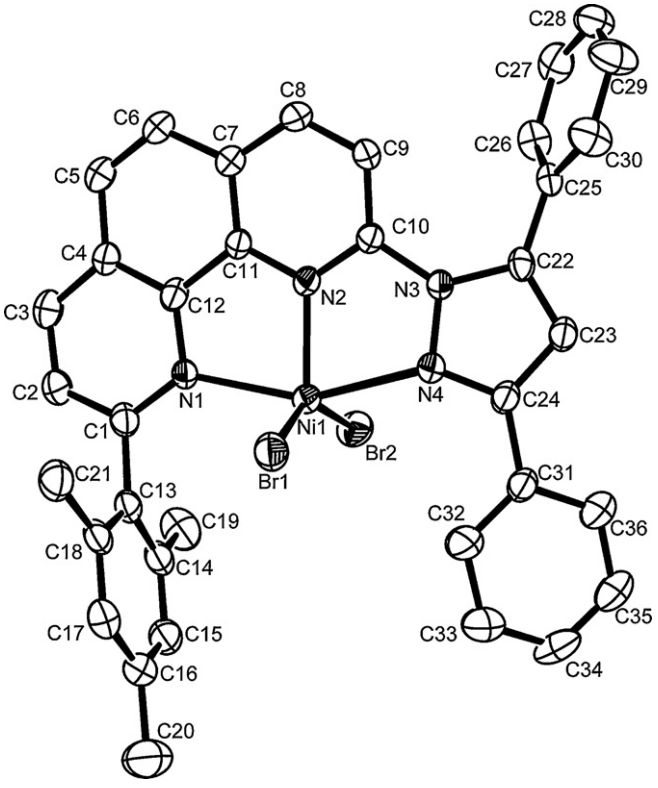

Fig. 2. The molecular structure of **12b** (thermal ellipsoids at the 30% probability level and hydrogen atoms are omitted for clarity).

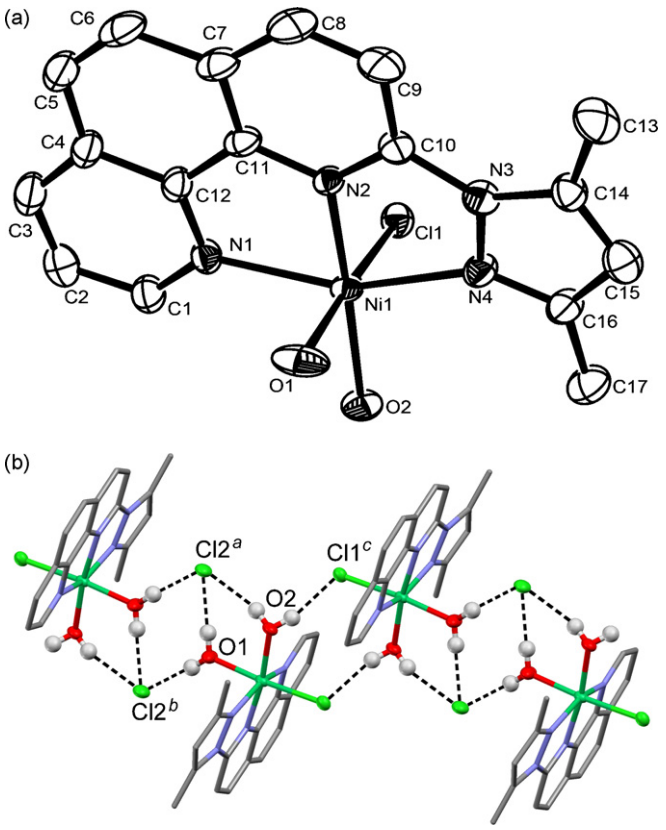

Fig. 3. (a) The molecular structure of the complex cation [NiCl(**L**^{1})$(H_2O)_2$]$^+$ in **1a**′; (b) hydrogen-bonded 1D zigzag chain in the crystal structure of **1a**′. Hydrogen bonding parameters O···Cl (Å), ∠O–H···Cl (°): O1 – H1C···Cl2^a: 3.075(3), 174(4); O1–H1B···Cl2^b: 3.065(3), 175(4); O2–H2C···Cl2^a: 3.195(3), 163(4); O2–H2B···Cl1^c: 3.104(3), 165(4). Symmetry code: ^{a} $x-1, y+1, z$; ^{b} $-x+1, -y+1, -z+1$; ^{c} $-x, -y+2, -z+2$.

get the desired composition of [$NiCl_2$(**L**^{1})] (**1a**), as confirmed by elemental analysis and IR spectroscopy.

2.3. Ethylene oligomerization by the N^N^N-coordinated nickel(II) complexes

The catalytic behavior of the complexes for ethylene oligomerization was investigated using MAO as cocatalyst, and all of the complexes displayed good catalytic activities (10^4 to 10^5 g mol^{-1} h^{-1}). The catalytic activities are readily compared to other nickel complexes incorporating tridentate ligands. For instance, the N^N^O [10] and N^O^N [11] complexes show activities of around 10^4 g mol^{-1} h^{-1} atm^{-1}, while the P^N^N catalysts [14] can reach 10^6 g mol^{-1} h^{-1} atm^{-1}. The ethylene reactivity of the N^N^N complexes [12,20] can be up to 10^5 g mol^{-1} h^{-1} atm^{-1}, which is similar to the nickel complexes presented in this work (the activity of complex **12a** is 14.7×10^4 g mol^{-1} h^{-1} atm^{-1}). In a routine scan of the effect of MAO, the optimum catalytic activity was observed at an Al/Ni molar ratio of 1500 (vide infra). Therefore, the oligomerization experiments were carried out with a fixed Al/Ni molar ratio of 1500, and the resultant data are summarized in Table 3.

2.3.1. Effects of the coordination environment

The coordination environment and substituents of the complexes showed different influences on their reactivity with ethylene. The Ni dichloride complexes (**1a–12a**) and the corresponding dibromide complexes (**1b–12b**) have similar oligomerization activities. As analyzed by GC and GC–MS, the major oligomeric products are ethylene dimers (1-butene and *trans*-2-butene) with a small

Table 3
Ethylene oligomerization by complexes **1a–12a** and **1b–12b**[a]

Entry	Cat.	Yield (g)	Activity (10^4 g mol^{-1} h^{-1})	α-Olefin [b] (%)	Oligomer distribution[b]	
					C4%	C6%
1	**1a**	0.08	3.10	>67	97.2	2.8
2	**2a**	0.09	3.72	>67	95.8	4.2
3	**3a**	0.12	4.97	>59	92.2	7.8
4	**4a**	0.10	4.55	>54	93.6	6.4
5	**5a**	0.20	7.86	>56	89.9	10.1
6	**6a**	0.24	9.42	>56	87.3	12.7
7	**7a**	0.19	7.60	>52	95.9	4.1
8	**8a**	0.22	8.96	>55	90.6	9.4
9	**9a**	0.26	10.2	>56	89.4	10.6
10	**10a**	0.20	7.78	>56	94.3	5.7
11	**11a**	0.24	9.51	>53	91.8	8.2
12	**12a**	0.37	14.7	>49	88.7	11.3
13	**1b**	0.07	3.03	>67	97.7	2.3
14	**2b**	0.09	3.46	>65	96.3	3.7
15	**3b**	0.12	4.75	>66	94.2	5.8
16	**4b**	0.10	4.06	>62	96.5	3.5
17	**5b**	0.16	6.58	>50	92.8	7.2
18	**6b**	0.21	8.33	>52	90.4	9.6
19	**7b**	0.18	7.08	>56	96.1	3.9
20	**8b**	0.21	8.46	>55	93.5	6.5
21	**9b**	0.23	9.29	>53	91.2	8.8
22	**10b**	0.18	7.10	>56	93.2	6.8
23	**11b**	0.22	8.81	>57	93.3	6.7
24	**12b**	0.32	12.7	>51	89.8	10.2

[a] Conditions: 5 μmol of catalyst, cocat MAO, Al/Ni = 1500, toluene 30 mL, 30 min, 1 atm, and 20 °C.
[b] Determined by GC and GC–MS.

amount of trimers (up to 12.7%, entry 6 in Table 3) including mainly 1-hexene, 2-hexene and trace of 3-methyl-1-pentene.

With β-H elimination assumed as the only chain-transfer mechanism in an insertion polymerization the probability α of chain growth calculates to $\alpha = k_w c_M/(k_w c_M + k_{\beta\text{-H}})$ with k_w = rate constant for propagation, c_M = concentration of monomer, and $k_{\beta\text{-H}}$ = rate constant for β-H elimination. It could be shown that the growth probability α decreases with increasing chain length for the first insertions, due to $k_w = f(P)$ and subsequently $\alpha = f(P)$ with P = degree of oligomerization. In order for a dimeric species (butene, $P = 2$) to be the major product (80–90 mol%, cf. Table 3) in ethylene oligomerization a very steep decrease of the insertion rate for the first (into Ni–H) over the second and all subsequent insertions has to be assumed together with the rate of the β-hydrogen elimination in the range of k_w. It was estimated that $k_w(P = 1)/k_w(P \geq 2) = 20$ and $k_{\beta\text{-H}}/k_w(P = 1) \approx 5$ for the predominant formation of a dimer [23].

The steric bulk of the ligands significantly affected the catalytic activity of the complexes. As shown in Table 3 and Fig. 4, increasing the size of the substituent R^1 on the 9-position of 1,10-phenanthroline and R^2 and R^3 on the pyrazolyl ring resulted in better catalytic activities of the complexes. The activity of [$NiCl_2$(L)] (series a) and [$NiBr_2$(L)] (series b) increased with larger R^1 substituent (H → Ph → 1-naphthyl → mesityl) for a given R^2 and R^3 combination. For example, there is a nearly 3-fold increase of activity for **12a** (R^1 = mesityl, Table 3, entry 12) compared to **3a** (R^1 = H, entry 3). With the same R^1 the activity also increased when the R^2 and R^3 groups became bulkier from **1**, **4**, **7**, and **10** (with $R^2 = R^3$ = Me) over **2**, **5**, **8**, and **11** (with R^2 = Me and R^3 = Ph) to **3**, **6**, **9**, and **12** (with $R^2 = R^3$ = Ph). Hence, complexes **12a** and **12b** that bear the bulkiest ligand, 2-(3,5-diphenylpyrazol-1-yl)-9-mesityl-1,10-phenanthroline (L^{12}), display the best catalytic activities (14.7 and 12.7 × 10^4 g mol(Ni)$^{-1}$ h^{-1}, respectively) among the two series of complexes.

The aryl groups can exert a conjugating effect which can stabilize the insertion transition state and thereby increase the activity, as seen before in polymerization reactions [24]. The increase of the activity could be attributed to the steric effects of the bulkier R substituents that can suppress chain-transfer reactions (typically β-H elimination) and therefore increase the activity [25]. Complexes with R^1 = aryl, $R^2 = R^3$ = Ph (**6**, **9**, and **12**) indeed gave the highest C_6 percentage in each $NiCl_2$ (**a**) and $NiBr_2$ (**b**) series. Still the C_6 percentage of around 10% and its increase from about 5% cannot alone account for the doubling or tripling of the yield and activity. We, therefore, suggest that the steric bulk of the aryl groups creates a reaction channel which makes the ethylene coordination to the Ni atom more efficient in terms of increasing the probability for insertion into the Ni–C or Ni–H bond and decreasing the probability for a re-dissociation (Scheme 2). Such an activity increase with increased steric bulk in a more directing environment has been observed in olefin polymerization reactions with zirconocene/MAO catalysts, elegantly exemplified in the so-called "advanced metallocenes" [26].

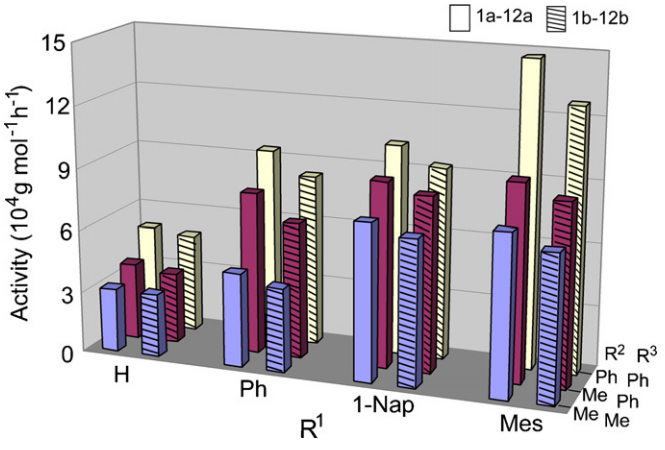

Fig. 4. Effects of the ligands on the activity of the precatalysts (**1a–12a**, **1b–12b**).

Table 4
Ethylene oligomerization with **12a** and **9a**/MAO under different conditions[a]

Entry	Al/Ni	T (°C)	Time (min)	Yield (g)	Activity (10^4 g mol^{-1} h^{-1})	α-Olefin[b] (%)	Oligomer distribution[b]	
							C4%	C6%
12a/MAO								
25	500	20	30	0.18	7.18	>55	94.9	5.1
26	1000	20	30	0.23	9.21	>53	91.3	8.7
27	2000	20	30	0.29	11.5	>59	90.5	9.5
28	2500	20	30	0.26	10.6	>65	93.8	6.2
29a	1500	20	15	0.34	27.6	>48	92.0	8.0
30a	1500	20	30	0.37	14.7	>49	88.7	11.3
31a	1500	20	45	0.37	9.93	>47	87.6	12.4
32a	1500	20	60	0.38	7.57	>45	86.4	13.6
33a	1500	20	90	0.39	5.25	>43	84.3	15.7
34	1500	20	120	0.40	4.02	>43	83.4	16.6
35	1500	0	30	0.23	9.09	>56	89.6	10.4
36	1500	40	30	0.44	17.6	>52	86.3	13.7
37	1500	60	30	0.26	10.4	>51	93.9	6.1
38	1500	80	30	0.19	7.45	>62	95.1	4.9
9a/MAO								
29b	1500	20	15	0.24	19.5	>57	91.7	8.3
30b	1500	20	30	0.26	10.2	>56	89.4	10.6
31b	1500	20	45	0.26	6.92	>54	88.1	11.9
32b	1500	20	60	0.27	5.31	>52	84.1	15.9
33b	1500	20	90	0.28	3.73	>50	82.4	17.6

[a] Conditions: 5 μmol catalyst, cocat MAO, toluene 30 mL, 1 atm.
[b] Determined by GC and GC-MS.

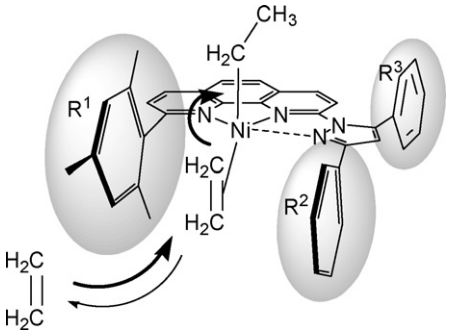

Scheme 2. Representation of the reaction channel formed through the bulky aryl groups (shaded areas) which renders the ethylene coordination more efficient towards C–C bond formation (bold arrows) and decreases the back reaction of dissociation (normal arrow).

2.3.2. Effects of Al/Ni molar ratio

The influence of MAO to metal molar ratio on ethylene activation was investigated in detail with **12a** in the range 500–2500 (entries 25–28 and 30a, Table 4). The catalytic activity first increased from an Al/Ni ratio of 500 to 1500, at which point the highest catalytic activity was attained (entry 12, Table 3). With further increasing the Al/Ni ratio from 1500 to 2500, the activity decreased slightly. On the other hand, varying the MAO to nickel ratio has little influence on the oligomer distribution.

2.3.3. Effects of oligomerization temperature and time

The catalytic lifetime of **12a** was investigated by varying the reaction time from 15 to 120 min (entries 29–33, Table 4). In the presence of MAO, ethylene was consumed very quickly over the first 15 min, and the highest activity of 2.76×10^5 g mol(Ni)$^{-1}$ h^{-1} was obtained during 15 min (entry 29a). Between 15 and 30 min the activity levelled off with only a low increase in yield from 15 to 120 min (entry 29a–34). With prolonged reaction time, the oligomerization yield increased only very slightly but the yield of C6 increased progressively, which could be attributed to the reinsertion of the 1-butene and 2-butene products to form *cis*-2-hexene and 3-methyl-1-pentene [27]. Notably, at 120 min, the complexes still showed some very low activity (small increase in yield from entry 33a–34). Time experiments carried out with the less active catalyst **9a**/MAO showed the same trend with the activity levelling off after 15 min, a low increase in yield from 15 to 90 min but progressive increase of C6 (entry 29b–33b).

The catalytic system of **12a** with 1500 equiv of MAO was investigated at different reaction temperatures under 1 atm of ethylene (entries 35–38 and 30a, Table 4). When the temperature was raised by every 20 °C from 0 to 80 °C, the catalytic activity of **12a** increased gradually, reaching the optimum value at 40 °C (entry 36). Upon

Table 5
Ethylene oligomerization with **12a** and **12b** at different pressures[a]

Entry	Cat.	P (atm)	Yield (g)	Activity (10^5 g mol^{-1} h^{-1})	α-Olefin [b] (%)	Oligomer distribution[b]	
						C4%	C6%
39	**12a**	5.0	1.05	2.09	>28	94.9	5.1
40	**12a**	7.5	1.28	2.56	>32	94.4	5.6
41	**12a**	10	1.51	3.01	>32	93.4	6.6
42	**12b**	5.0	0.80	1.59	>31	96.3	3.7
43	**12b**	7.5	0.97	1.94	>28	94.5	5.5
44	**12b**	10	1.22	2.44	>29	92.8	7.2

[a] Conditions: 5 μmol catalyst, cocat MAO, Al/M = 1500, toluene 100 mL, 60 min, and 20 °C.
[b] Determined by GC and GC–MS.

further elevation of the temperature to 60 and 80 °C, the catalytic activity began to decrease. This could be due to the thermal instability of the active species at higher temperature. However, part of the activity decrease by ~50% from 40 °C (entry 36, Table 4) to 80 °C (entry 38, Table 4) can also be ascribed to the decrease of ethylene solubility, that is, monomer concentration in toluene which is 0.12 mol kg^{-1} bar^{-1} at 40 °C and 0.08 mol kg^{-1} bar^{-1} at 70 °C [28].

2.3.4. Effects of ethylene pressure on the catalytic activity

Ethylene oligomerization experiments with the nickel dichloro- (**12a**) and dibromo complexes (**12b**) were carried out under different pressures of ethylene, as shown in Table 5. The catalytic activities of the precatalysts **12a** and **12b** (entries 39–41 and 42–44) are only slightly enhanced at higher pressure of ethylene, and the nickel dichloride complexes are better than the dibromide analogs. However, elevation of ethylene pressure significantly increased the activities of the nickel complexes with bidentate (NˆN) 2,9-diaryl-1,10-phenanthrolines [18]. The best catalytic activity at 10 atm of ethylene was obtained with **12a** (3.01×10^5 g mol(Ni)$^{-1}$ h^{-1}). The results also indicate that the effects of the ligand environment on the activity at 10 atm is similar to those observed at 1 atm of ethylene.

3. Conclusions

A series of nickel complexes bearing 2-pyrazolyl substituted 1,10-phenanthroline derivatives have been synthesized and characterized. These complexes exhibit good activities for ethylene oligomerization in the presence of MAO as cocatalyst, and the main products are ethylene dimers and trimers. In the tridentate NˆNˆN catalytic system, complexes containing bulky aryl substituents have higher ethylene activity. The ethylene oligomerization activities are influenced by the Al/M molar ratio, reaction time, reaction temperature and ethylene pressure, and complex **12a** displays the best catalytic activity among the series of complexes (up to 3.01×10^5 g mol(Ni)$^{-1}$ h^{-1} at 10 atm). The increase of the activity and the C_6-percentage with the steric bulk of the ligand suggests continuing along this route with the addition of even bulkier groups in the 9-position of the phenanthroline ring and the 3- and 5-position of the pyrazolyl ring to improve the catalytic behavior.

4. Experimental

4.1. General considerations

All air- and water-sensitive reactions were performed under nitrogen using standard Schlenk techniques. THF and Et_2O were dried by sodium/benzophenone and distilled under nitrogen prior to use. Toluene was dried by sodium. MAO solution (1.65 M in toluene) was purchased from Albemarle Co. (USA). ^1H and ^{13}C NMR spectra were obtained on a Mercury plus-400 spectrometer with TMS as the internal standard. IR spectra were recorded as KBr pellets with a Bruker IFS 120HR spectrometer. ESI-MS spectra were measured on a Waters ZQ 4000 instrument. Element analyses were performed with an Elementar VarioEL instrument.

1,10-Phenanthroline, bromobenzene, 1-bromonaphthalene, acetylacetone, 2-bromomesitylene, and other common chemicals were commercially available and were used without further purification. Benzoylacetone [29] and dibenzoylmethane [30] were synthesized according to literature procedures. 2-Phenyl-1,10-phenanthroline, 2-(1-naphthyl)-1,10-phenanthroline, 2-(2,4,6-trimethylphenyl)-1,10-phenanthroline [31], and 2-hydrazine-1,10-phenanthroline [21] were prepared as described in the literature.

4.2. Synthesis of the ligands L^1–L^{12}

The compound 2-(3,5-dimethylpyrazol-1-yl)-1,10-phenanthroline (ligand L^1) is known [21]. The new analogs (L^2–L^{12}) were prepared using slightly modified procedures: a mixture of 2-hydrazine-1,10-phenanthroline or 2-hydrazine-9-aryl-1,10-phenanthroline (3.0 mmol) and the diketone (3.6 mmol), i.e. acetylacetone (for L^1, L^4, L^7, and L^{10}), benzoylacetone (for L^2, L^5, L^8, and L^{11}), or dibenzoylmethane (for L^3, L^6, L^9, and L^{12}), was stirred in dry methanol (15 mL) containing a few drops of acetic acid for 6–12 h. The solvent was removed and the residue was recrystallized from chloroform/activated charcoal to give the products.

4.2.1. 2-(3,5-Dimethylpyrazol-1-yl)-1,10-phenanthroline (L^1)

White solid (79%). mp: 161 °C. ESI-MS: *m/z* 275.3 $[M+H]^+$. ^1H NMR (400 MHz, $CDCl_3$, δ/ppm): 9.16 (dd, *J* = 1.6, 4.4 Hz, 1H, H-9), 8.35–8.25 (m, 3H, H-8, H-4, H-7), 7.83–7.76 (m, 2H, H-5, H-6), 7.64 (dd, *J* = 8.0, 4.4 Hz, 1H, H-3), 6.09 (s, 1H, pyrazolyl-H), 3.02 (s, 3H, CH_3), and 2.35 (s, 3H, CH_3). Anal. Calcd for $C_{17}H_{14}N_4$: C 74.43, H 5.14, N 20.42; Found C 74.31, H 5.19, and N 20.48%.

4.2.2. 2-(3-Methyl-5-phenylpyrazol-1-yl)-1,10-phenanthroline (L^2)

Pale yellow solid (67%). mp: 174–175 °C. ESI-MS: *m/z* 337.3 $[M+H]^+$. ^1H NMR: 9.10 (dd, *J* = 1.6, 4.4 Hz, 1H, H-9), 8.23 (dd, *J* = 1.6, 8.0 Hz, 1H, H-7), 8.16 (d, *J* = 8.0 Hz, 1H, H-4), 7.80–7.75 (m, *J* = 9.2 Hz, 2H, H-5, H-6), 7.60 (dd, *J* = 4.4, 8.0 Hz, 1H, H-8), 7.42 (d, *J* = 8.0 Hz, 1H, H-3), 7.40 (m, 2H, Ph-*o*-H), 7.28 (m, 3H, Ph-H), 6.39 (s, 1H, H-4′), and 2.46 (s, 3H, CH_3). Anal. Calcd for $C_{22}H_{16}N_4$: C 78.55, H 4.79, N 16.66; Found C 78.47, H 4.69, and N 16.82%.

4.2.3. 2-(3,5-Diphenylpyrazol-1-yl)-1,10-phenanthroline (L^3)

Pale yellow solid (63%). mp: 187–188 °C. ESI-MS: *m/z* 399.4 $[M+H]^+$. ^1H NMR: 9.08 (dd, *J* = 1.6, 4.4 Hz, 1H, H-9), 8.24 (dd, *J* = 8.8, 1.6 Hz, 2H, H-4, H-7), 8.03–8.01 (t, *J* = 1.2, 7.2 Hz, 2H, Ph-*o*-H), 7.79 (s, 2H, H-5, H-6), 7.73 (d, *J* = 8.4 Hz, 1H, H-8), 7.61 (dd, *J* = 4.4, 8.0 Hz, 1H, H-3), 7.50–7.46 (m, 5H, Ph-H), 7.44–7.31 (m, 5H, Ph-H), and 6.92 (s, 1H, H-4′). Anal. Calcd for $C_{27}H_{18}N_4$: C 81.39, H 4.55, N 14.06; Found C 81.37, H 4.32, and N 13.87%.

4.2.4. 2-(3,5-Dimethylpyrazol-1-yl)-9-phenyl-1, 10-phenanthroline (L^4)

White solid (66%). mp: 154–155 °C. ESI-MS: *m/z* 351.2 $[M+H]^+$. ^1H NMR: 8.41–8.39 (m, 5H, Ph-*o*-H, H-4, H-7, H-8), 8.14 (d, *J* = 8.4 Hz, 1H, H-3), 7.81 (s, 2H, H-5, H-6), 7.58–7.49 (m, 3H, Ph-H), 6.13 (s, 1H, H-4′), 3.26 (s, 3H, CH_3), and 2.37 (s, 3H, CH_3). Anal. Calcd for $C_{23}H_{18}N_4$: C 78.83, H 5.18, N 15.99; Found C 78.84, H 5.06, and N 15.75%.

4.2.5. 2-(3-Methyl-5-phenylpyrazol-1-yl)-9-phenyl-1,10-phenanthroline (L^5)

Pale yellow solid (61%). mp: 197–198 °C. ESI-MS: *m/z* 413.4 $[M+H]^+$. ^1H NMR: 8.35 (d, *J* = 8.8 Hz, 1H, H-4), 8.24 (d, *J* = 8.4 Hz, 1H, H-7), 8.09 (d, *J* = 8.0 Hz, 1H, H-8), 8.02 (d, *J* = 8.8 Hz, 1H, H-3), 7.92–7.90 (dd, *J* = 1.6, 6.8 Hz, 2H, Ph-*o*-H), 7.77 (s, 2H, H-5, H-6), 7.58 (d, *J* = 7.2 Hz, 2H, Ph-*o*-H), 7.49–7.44 (m, 3H, Ph-H), 7.34–7.27 (m, 3H, Ph-H), 6.43 (s, 1H, H-4′), and 2.44 (s, 3H, CH_3). Anal. Calcd for $C_{28}H_{20}N_4$: C 81.53, H 4.89, N 13.58; Found: C 81.46, H 4.92, and N 13.47%.

*4.2.6. 2-(3,5-Diphenylpyrazol-1-yl)-9-phenyl-1,10-phenanthroline (**L⁶**)*

Pale yellow solid (56%). mp: 204–205 °C. ESI-MS: *m/z* 475.4 $[M+H]^+$. ^{1}H NMR: 8.35 (d, *J* = 8.4 Hz, 1H, H-4), 8.27–8.23 (t, *J* = 8.8 Hz, 2H, Ph-H), 8.04–7.98 (m, 3H, H-3, H-7, H-8), 7.93–7.91 (m, 2H, Ph-*o*-H), 7.79 (s, 2H, H-5, H-6), 7.68 (dd, *J* = 7.2, 1.2 Hz, 2H, Ph-*m*-H), 7.51–7.45 (m, 5H, Ph-H), 7.39–7.27 (m, 5H, Ph-H), and 6.94 (s, 1H, H-4′). Anal. Calcd for $C_{33}H_{22}N_4$: C 83.52, H 4.67, N 11.81; Found C 83.43, H 4.43, and N 11.55%.

*4.2.7. 2-(3,5-Dimethylpyrazol-1-yl)-9-(1-naphthyl)-1,10-phenanthroline (**L⁷**)*

Pale yellow solid (57%). mp: 178–179 °C. ESI-MS: *m/z* 401.3 $[M+H]^+$. ^{1}H NMR: 8.69 (d, *J* = 8.4 Hz, 1H, H-4), 8.40–8.30 (m, 3H, Nap-H, H-7), 8.00-7.95 (m, 3H, Nap-H, H-8), 7.84 (d, *J* = 4.4 Hz, 3H, H-5, H-6, H-3), 7.64–7.47 (m, 3H, Nap-H), 6.00 (s, 1H, H-4′), 2.93 (s, 3H, CH_3), and 2.32 (s, 3H, CH_3). Anal. Calcd for $C_{27}H_{20}N_4$: C 80.97, H 5.03, N 13.99; Found C 80.90, H 4.74, and N 13.76%.

*4.2.8. 2-(3-Methyl-5-phenylpyrazol-1-yl)]-9-(1-naphthyl)-1,10-phenanthroline (**L⁸**)*

Pale yellow solid (52%). mp: 181–182 °C. ESI-MS: *m/z* $[M+H]^+$ 463.4. ^{1}H NMR: 8.29 (dd, *J* = 8.8, 8.0 Hz, 2H, Nap-H), 8.02 (d, *J* = 8.4 Hz, H-4), 7.95 (t, *J* = 7.4 Hz, 3H, H-7, Nap-H), 7.88–7.80 (m, 3H, H-5, H-6, H-8), 7.65–7.56 (m, 2H, H-3, Nap-H), 7.52–7.40 (m, 4H, Nap-H, 2Ph-H), 7.06 (t, *J* = 7.6 Hz, 2H, Ph-H), 6.99 (t, *J* = 7.4 Hz, 1H, Ph-H), 6.31 (s, 1H, H-4′), and 2.39 (s, 3H, CH_3). Anal. Calcd for $C_{32}H_{22}N_4$: C 83.09, H 4.79, N 12.11; Found C 83.30, H 4.74, and N 11.94%.

*4.2.9. 2-(3,5-Diphenylpyrazol-1-yl)-9-(1-naphthyl)-1,10-phenanthroline (**L⁹**)*

Pale yellow solid (42%). mp: 189–190 °C. ESI-MS: *m/z* 525.7 $[M+H]^+$. ^{1}H NMR: 8.37 (d, *J* = 8.8 Hz, 2H, Nap-H), 8.29 (d, *J* = 8.0 Hz, 2H, Nap-H), 8.14 (d, *J* = 8.8 Hz, H-4), 8.07 (d, *J* = 8.0 Hz, H-7), 7.97 (t, *J* = 7.6 Hz, 4H, H-5, H-6, H-3, H-8), 7.88 (t, *J* = 7.6 Hz, 3H, Nap-H), 7.65 (t, *J* = 7.8 Hz, 3H, Nap-H), 7.57–7.37 (m, 7H, Ph-H, Nap-H), 7.34 (t, *J* = 7.0 Hz, 1H, Ph-H), 7.09 (t, *J* = 7.6 Hz, 2H, Ph-H), 7.00 (t, *J* = 7.2 Hz, 1H, Ph-H), and 6.83 (s, 1H, H-4′). Anal. Calcd for $C_{37}H_{24}N_4$: C 84.71, H 4.61, N 10.68; Found C 85.02, H 4.38, and N 10.39%.

*4.2.10. 2-(3,5-Dimethylpyrazol-1-yl)-9-mesityl-1,10-phenanthroline (**L¹⁰**)*

Pale yellow solid (52%). mp: 219–220 °C. ESI-MS: *m/z* 393.5 $[M+H]^+$. ^{1}H NMR: 8.28 (m, 3H, H-4, H-7, H-8), 7.81 (s, 2H, H-5, H-6), 7.59 (d, *J* = 8.0 Hz, 1H, H-3), 6.98 (s, 2H, Ph-*m*-H), 6.02 (s, 1H, H-4′), 2.91 (s, 3H, CH_3), 2.36 (s, 3H, CH_3), 2.32 (s, 3H, CH_3), and 2.18 (s, 6H, CH_3). Anal. Calcd for $C_{26}H_{24}N_4$: C 79.56, H 6.16, N 14.27; Found C 79.27, H 6.14, and N 13.81%.

*4.2.11. 2-(3-Methyl-5-phenylpyrazol-1-yl)-9-mesityl-1,10-phenanthroline (**L¹¹**)*

Pale yellow solid (48%). mp: 202–203 °C. ESI-MS: *m/z* 455.4 $[M+H]^+$. ^{1}H NMR: 8.27 (d, *J* = 8.8 Hz, H-4), 8.35 (d, *J* = 8.0 Hz, H-7), 7.81 (t, *J* = 4.8 Hz, 3H, H-5, H-6, H-8), 7.51 (d, *J* = 7.84 Hz, 1H, H-3), 7.42 (m, 2H, Ph-H), 7.08 (d, *J* = 2.8 Hz, 3H, Ph-*o*-H, Ph-*p*-H), 6.96 (s, 2H, Mes-ArH), 6.32 (s, 1H, H-4′), 2.39 (s, 3H, CH_3), 2.37 (s, 3H, CH_3), 2.25 (s, 3H, CH_3), and 1.96 (s, 3H, CH_3). Anal. Calcd for $C_{31}H_{26}N_4$: C 81.90, H 5.70, N, 12.33; Found C 81.75, H 5.44, and N 12.55%.

*4.2.12. 2-(3,5-Diphenylpyrazol-1-yl)-9-mesityl-1,10-phenanthroline (**L¹²**)*

Pale yellow solid (41%). mp: 192 °C. ESI-MS: *m/z* 517.4 $^+$. ^{1}H NMR: 8.35 (d, *J* = 8.8 Hz, 1H, H-4), 8.23 (d, *J* = 8.0 Hz, 1H, H-7), 8.06 (d, *J* = 8.4 Hz, 1H, H-8), 7.96 (dd, *J* = 1.6, 6.8 Hz, 2H, H-3), 7.83 (s, 2H, H-5, H-6), 7.53–7.50 (m, 3H, Ph-H), 7.44 (t, *J* = 7.4 Hz, 2H), 7.35 (t, *J* = 7.4 Hz, 1H, Ph-H), 7.09–7.07 (m, 3H, Ph-H, Mes-ArH), 6.97 (s, 1H, Mes-ArH), 6.83 (s, 1H, H-4′), 2.38 (s, 3H, CH_3), and 1.97 (s, 6H, CH_3). Anal. Calcd for $C_{36}H_{28}N_4$: C 83.69, H 5.46, N 10.84; Found C, 83.45, H 5.51, and N 10.95%.

4.3. Synthesis of the nickel complexes

The nickel(II) complexes were synthesized by the following general procedure: a solution of the ligand in THF was added to an equimolar amount of $NiCl_2{\cdot}6H_2O$ or $NiBr_2{\cdot}6H_2O$ in THF. The reaction mixture was stirred at room temperature for 12 h. The resultant precipitate was collected, washed with THF and diethyl ether, and dried in vacuum. All of the complexes were prepared in high yield in this manner.

[$NiCl_2$(L¹)] (1a). Light green powder (96.9%). Mp: > 300 °C. IR (KBr, ν/cm^{-1}): 3050, 2919, 1613, 1584, 1569, 1459, 1432, 1416, 1385, 1367, 1332, 1128, 1070, 985, 848, 757, 734, and 649. Anal. Calcd for $C_{17}H_{14}N_4NiCl_2$ (403.92): C 50.55, H 3.49, N 13.87; Found: C 50.36, H 3.28, and N 13.48%.

[$NiCl_2$(L²)] (2a). Light green powder (97.2%). Mp: > 300 °C. IR (KBr, ν/cm^{-1}): 3055, 2921, 1611, 1563, 1463, 1431, 1403, 1363, 1329, 1201, 1141, 1032, 978, 885, 854, 776, 764, 738, 702, and 649. Anal. Calcd for $C_{22}H_{16}N_4NiCl_2$ (465.99): C 56.70, H 3.46, N 12.02; Found: C 56.92, H 3.54, and N 11.77%.

[$NiCl_2$(L³)] (3a). Light green powder (94.0%). Mp: > 300 °C. IR (KBr, ν/cm^{-1}): 3053, 2920, 2871, 1613, 1588, 1558, 1497, 1462, 1433, 1404, 1332, 1152, 977, 851, 761, 733, 700, and 651. Anal. Calcd for $C_{27}H_{18}N_4NiCl_2$ (528.06): C 61.41, H 3.44, N 10.61; Found: C 61.02, H 3.25, and N 10.25%.

[$NiCl_2$(L⁴)] (4a). Yellow powder (93.4%). Mp: > 300 °C. IR (KBr, ν/cm^{-1}): 3051, 2920, 1621, 1578, 1561, 1499, 1443, 1425, 1364, 1336, 1131, 984, 858, 778, 740, 704, and 655. Anal. Calcd for $C_{23}H_{18}N_4NiCl_2$ (480.01): C 57.55, H 3.78, N 11.67; Found: C 57.21, H 3.90, and N 11.49%.

[$NiCl_2$(L⁵)] (5a). Yellow powder (92.2%). Mp: > 300 °C. IR (KBr, ν/cm^{-1}): 3053, 2923, 2853, 1622, 1593, 1574, 1510, 1498, 1443, 1426, 1380, 1363, 1335, 1143, 1034, 978, 860, 760, 741, 701, and 654. Anal. Calcd for $C_{28}H_{20}N_4NiCl_2$ (542.08): C 62.04, H 3.72, N 10.34; Found: C 62.36, H 3.58, and N 10.03%.

[$NiCl_2$(L⁶)] (6a). Yellow powder (93.0%). Mp: > 300 °C. IR (KBr, ν/cm^{-1}): 3055, 2922, 2852, 1622, 1611, 1593, 1571, 1497, 1457, 1426, 1363, 1337, 1154, 979,862, 771, 761, 740, 701, and 657. Anal. Calcd for $C_{33}H_{22}N_4NiCl_2$ (604.15): C 65.60, H 3.67, N 9.27; Found: C 65.98, H 3.82, and N 9.13%.

[$NiCl_2$(L⁷)] (7a). Light yellow powder (95.3%). Mp: > 300 °C. IR (KBr, ν/cm^{-1}): 3050, 2922, 2853, 1621, 1580, 1560, 1499, 1456, 1425, 1362, 1336, 983, 860, 781, 757, and 664. Anal. Calcd for $C_{27}H_{20}N_4NiCl_2$ (530.07): C 61.18, H 3.80, N 10.57; Found: C 60.90, H 3.62, and N 10.41%.

[$NiCl_2$(L⁸)] (8a). Light yellow powder (93.0%). Mp: > 300 °C. IR (KBr, ν/cm^{-1}): 3054, 2924, 1623, 1591, 1577, 1499, 1442, 1426, 1360, 1336, 972, 900, 864, 782, 761, and 701. Anal. Calcd for $C_{32}H_{22}N_4NiCl_2$ (592.14): C 64.91, H 3.74, N 9.46; Found: C 64.97, H 4.02, and N 9.52%.

[$NiCl_2$(L⁹)] (9a). Yellow powder (90.4%). Mp: > 300 °C. IR (KBr, ν/cm^{-1}): 3055, 2923, 2853, 1622, 1592, 1575, 1495, 1458, 1426, 1362, 1336, 973, 901, 863, 774, and 700. Anal. Calcd for $C_{37}H_{24}N_4NiCl_2$ (654.21): C 67.93, H 3.70, N 8.56; Found: C 68.17, H 3.49, and N 8.51%.

[$NiCl_2$(L¹⁰)] (10a). Light yellow powder (92.8%). Mp: > 300 °C. IR (KBr, ν/cm^{-1}): 3054, 2920, 2854, 1615, 1580, 1562, 1505, 1457, 1425, 1365, 1335, 987, 897, 858, 775, 751, and 701. Anal. Calcd for $C_{26}H_{24}N_4NiCl_2$ (522.09): C 59.81, H 4.63, N 10.73; Found: C 59.51, H 4.67, and N 10.36%.

[$NiCl_2(L^{11})$] (11a). Light yellow powder (91.9%). Mp: > 300 °C. IR (KBr, ν/cm^{-1}): 3050, 2921, 2855, 1615, 1577, 1497, 1451, 1427, 1364, 1336, 980, 895, 858, 758, and 701. Anal. Calcd for $C_{31}H_{26}N_4NiCl_2$ (584.16): C 63.74, H 4.49, N 9.59; Found: C 63.55, H 4.51, and N 9.34%.

[$NiCl_2(L^{12})$] (12a). Yellow powder (92.0%). Mp: > 300 °C. IR (KBr, ν/cm^{-1}): 3054, 2921, 2858, 1612, 1573, 1493, 1457, 1427, 1361, 1336, 979, 895, 864, 771, 759, and 703. Anal. Calcd for $C_{36}H_{28}N_4NiCl_2$ (646.23): C 66.91, H 4.37, N 8.67; Found: C 67.28, H 4.34, and N 8.90%.

[$NiBr_2(L^1)$] (1b). Pale blue powder (95.5%). Mp: > 300 °C. IR (KBr, ν/cm^{-1}): 3056, 2924, 1613, 1585, 1571, 1504, 1459, 1432, 1416, 1384, 1366, 1352, 1330, 1128, 1070, 984, 846, 786, 755, 733 680, and 650. Anal. Calcd for $C_{17}H_{14}N_4NiBr_2$ (492.82): C 41.43, H 2.86, N 11.37; Found: C 40.91, H 2.64, and N 11.20%.

[$NiBr_2(L^2)$] (2b). Pale blue powder (94.3%). Mp: > 300 °C. IR (KBr, ν/cm^{-1}): 3059, 2928, 1611, 1589, 1566, 1510, 1462, 1431, 1407, 1377, 1350, 1199, 1142, 1031, 976, 885, 853, 763, 736, 703, and 650. Anal. Calcd for $C_{22}H_{16}N_4NiBr_2$ (554.89): C 47.62, H 2.90, N 10.10; Found: C 47.29, H 3.13, and N 9.89%.

[$NiBr_2(L^3)$] (3b). Pale blue powder (90.5%). Mp: > 300 °C. IR (KBr, ν/cm^{-1}): 3055, 2924, 1609, 1587, 1561, 1499, 1430, 1405, 1346, 1225, 1163, 1062, 1028, 975, 852, 764, 755, 735, 695, and 650. Anal. Calcd for $C_{27}H_{18}N_4NiBr_2$ (616.96): C 52.56, H 2.94, N 9.08; Found: C 52.25, H 3.10, and N 8.70%.

[$NiBr_2(L^4)$] (4b). Yellow powder (92.1%). Mp: > 300 °C. IR (KBr, ν/cm^{-1}): 3050, 2919, 1621, 1578, 1499, 1443, 1425, 1363, 1337, 1156, 1130, 983, 858, 777, 740, 707, 688, and 655. Anal. Calcd for $C_{23}H_{18}N_4NiBr_2$ (568.92): C 48.56, H 3.19, N 9.85; Found: C 48.02, H 2.80, and N 9.39%.

[$NiBr_2(L^5)$] (5b). Dark yellow powder (90.4%). Mp: > 300 °C. IR (KBr, ν/cm^{-1}): 3056, 2923, 2852, 1622, 1613, 1593, 1576, 1510, 1499, 1443, 1426, 1381, 1364, 1337, 1201, 1143, 1034, 860, 761, 701, and 654. Anal. Calcd for $C_{28}H_{20}N_4NiBr_2$ (630.99): C 53.30, H 3.19, N 8.88; Found: C 52.93, H 2.87, and N 9.03%.

[$NiBr_2(L^6)$] (6b). Dark yellow powder (89.6%). Mp: > 300 °C. IR (KBr, ν/cm^{-1}): 3054, 2923, 2852, 1621, 1610, 1591, 1571, 1496, 1459, 1425, 1363, 1337, 1151, 1068, 979, 859, 761, 739, 699, and 657. Anal. Calcd for $C_{33}H_{22}N_4NiBr_2$ (693.06): C 57.19, H 3.20, N 8.08; Found: C 57.51, H 3.10, and N 8.49%.

[$NiBr_2(L^7)$] (7b). Pale blue powder (94.7%). Mp: > 300 °C. IR (KBr, ν/cm^{-1}): 3050, 2922, 2851, 1623, 1580, 1560, 1501, 1425, 1363, 1337, 987, 860, 806, 781, 757, and 664. Anal. Calcd for $C_{27}H_{20}N_4NiBr_2$ (618.98): C 52.39, H 3.26, N 9.05; Found: C 52.68, H 3.39, and N 9.17%.

[$NiBr_2(L^8)$] (8b). Pale blue powder (93.0%). Mp: > 300 °C. IR (KBr, ν/cm^{-1}): 3050, 2924, 1621, 1610, 1590, 1577, 1498, 1426, 1360, 1335, 972, 900, 866, 781, 761, and 701. Anal. Calcd for $C_{32}H_{22}N_4NiBr_2$ (681.05): C 56.43, H 3.26, N 8.23; Found: C 56.49, H 3.19, and N 8.13%.

[$NiBr_2(L^9)$] (9b). Dark yellow powder (90.2%). Mp: > 300 °C. IR (KBr, ν/cm^{-1}): 3054, 2923, 2852, 1617, 1592, 1575, 1496, 1458, 1428, 1362, 1336, 972, 901, 862, 773, and 699. Anal. Calcd for $C_{37}H_{24}N_4NiBr_2$ (743.11): C 59.80, H 3.26, N 7.54; Found: C 59.69, H 3.10, and N 7.35%.

[$NiBr_2(L^{10})$] (10b). Pale blue powder (93.5%). Mp: > 300 °C. IR (KBr, ν/cm^{-1}): 3058, 2921, 2855, 1613, 1581, 1562, 1499, 1459, 1426, 1367, 1337, 987, 898, 863, 775, and 696. Anal. Calcd for $C_{26}H_{24}N_4NiBr_2$ (611.00): C 51.11, H 3.96, N 9.17; Found: C 51.10, H 3.79, and N 8.94%.

[$NiBr_2(L^{11})$] (11b). Pale blue powder (92.8%). Mp: > 300 °C. IR (KBr, ν/cm^{-1}): 3050, 2923, 2853, 1611, 1592, 1578, 1496, 1454, 1428, 1365, 1337, 980, 895, 858, 759, and 699. Anal. Calcd for $C_{31}H_{26}N_4NiBr_2$ (673.07): C 55.32, H 3.89, N 8.32; Found: C 55.35, H 3.88, and N 8.11%.

[$NiBr_2(L^{12})$] (12b). Pale blue powder (91.1%). Mp: > 300 °C. IR (KBr, ν/cm^{-1}): 3056, 2919, 1612, 1592, 1573, 1493, 1457, 1430, 1359, 1337, 979, 892, 860, 766, and 701. Anal. Calcd for $C_{36}H_{28}N_4NiBr_2$ (735.14): C 58.82, H 3.84, N 7.62; Found: C 59.14, H 3.68, and N 7.59%.

4.4. General procedure for ethylene oligomerization

4.4.1. Oligomerization at 1 atm

In a typical experiment, the complex (5 μmol) was added to a glass reactor, which was evacuated and filled three times with nitrogen and once with ethylene. Then 30 mL of freshly distilled toluene was introduced into the reactor with stirring. Methylaluminoxane toluene solution of desired amount was injected into the suspension via a syringe and the color of the solution changed immediately from colorless to yellow. After the reaction mixture was stirred under 1 atm of ethylene for a given period using a water bath to maintain the temperature, a small amount of the solution was taken out with a syringe and quenched by ice-cooled 10% HCl solution (ice-bath was used in order to prevent the loss of more volatile C_4). About 1 mL of the organic layer was dried with anhydrous $MgSO_4$ for GC or GC–MS measurements. Then the reaction was terminated by adding HCl/EtOH solution and no polymer was found.

4.4.2. High-pressure oligomerization

A 1L stainless-steel autoclave equipped with an electronically controlled stirrer was evacuated and filled three times with nitrogen and twice with ethylene. Freshly distilled toluene (100 mL) was added. After the temperature reached a certain point, MAO was injected followed by a toluene (20 mL) solution of the catalyst. The reactor pressure was kept constant throughout the oligomerization process by manually controlled addition of ethylene. After 30 min the reactor was cooled in an ice bath, the extra ethylene was vented off and the run was quenched with a solution of 10% HCl. Quantitative GC analysis of the product was performed immediately after the termination of the reaction.

GC analysis was performed with an SP-2100 gas chromatography spectrometer equipped with a flame ionization detector and an SE-30 silica capillary column. The column temperature was started at 50 °C (3 min), raised by 5 °C/min to 250 °C and kept at 250 °C for 10 min. GC–MS analysis was done using an Agilent 6890N/5973N GC/MS spectrometer with an HP-1 capillary column. The column temperature was started at 50 °C (2 min), raised by 15 °C/min to 280 °C and kept at 280 °C for 10 min. The yield of the oligomers was calculated by referencing to the mass of the used solvent based on the prerequisite that the mass of each fraction is approximately proportional to its integrated areas in the GC trace.

4.5. X-ray crystal structure determination

Diffraction data for the complexes were collected on a Bruker SMART APEX II diffractometer at room temperature (293 K) with graphite-monochromated Mo Kα radiation (λ = 0.71073 Å). An empirical absorption correction using SADABS [32] was applied for all data. The structures were solved by direct methods using the SHELXS program [33]. All non-hydrogen atoms were refined anisotropically by full-matrix least-squares on F^2 by the use of the program SHELXL [33]. The hydrogen atoms bonded to carbon were included in idealized geometric positions with thermal parameters equivalent to 1.2 times those of the atom to which they were attached. Hydrogen atoms on water were located from the difference Fourier map with O-H ≈0.85(1) Å and were refined isotropically with U(H) = 0.08 Å^2. Crystallographic data for the complexes **1a′**, **10b** and **12b** are listed in Table 6.

Table 6
Crystallographic data and structure refinement details

Complex	**1a**′	**10b**	**12b**·CH_2Cl_2
Empirical formula	$C_{17}H_{18}Cl_2N_4NiO_2$	$C_{26}H_{24}Br_2N_4Ni$	$C_{37}H_{30}Br_2Cl_2N_4Ni$
Fw	439.96	611.02	820.08
Crystal color	green	violet	yellow
Crystal system	triclinic	monoclinic	rhombohedral
Space group	$P\bar{1}$	$P2_1/c$	$R\bar{3}$
a (Å)	8.424(1)	10.0695(8)	22.159(1)
b (Å)	10.790(1)	13.960(1)	22.159(1)
c (Å)	11.486(1)	17.544(2)	22.159(1)
α (°)	76.113(2)	90	116.196(1)
β (°)	77.981(2)	98.341(4)	116.196(1)
γ (°)	68.50(1)	90	116.196(1)
V (Å^3)	934.6 (2)	2440.0(3)	5367.4(5)
Z	2	4	6
D_{calcd} (g cm^{-3})	1.563	1.663	1.522
F (0 0 0)	452	1224	2472
μ (mm^{-1})	1.34	4.09	2.957
Crystal size (mm^3)	0.33 × 0.19 × 0.12	0.26 × 0.24 × 0.23	0.36 × 0.30 × 0.26
θ range (°)	1.84–25.10	1.87–26.80	1.67–28.34
Reflections collected	4605	14196	33105
Unique reflections	3249	5194	8550
Goodness of fit on F^2	1.317	0.991	0.971
R^1, wR^2 ($I > 2\sigma(I)$)	0.0425, 0.0998	0.0437, 0.0891	0.0500, 0.1234
R^1, wR^2 (all data)	0.0582, 0.1070	0.0884, 0.1034	0.1380, 0.1551

Acknowledgements

This work was supported by the "Bairen Jihua" project of the Chinese Academy of Sciences and by the University of Freiburg.

References

[1] (a) C. Janiak, F. Blank, Macromol. Symp. 236 (2006) 14–22;
(b) C. Janiak, Coord. Chem. Rev. 250 (2006) 66–94.
[2] (a) F. Speiser, P. Braunstein, L. Saussine, Acc. Chem. Res. 38 (2005) 784–793;
(b) C. Bianchini, G. Giambastiani, I.G. Rios, G. Mantovani, A. Meli, A.M. Segarra, Coord. Chem. Rev. 250 (2006) 1391–1418.
[3] (a) L.K. Johnson, C.M. Killian, M. Brookhart, J. Am. Chem. Soc. 117 (1995) 6414–6415;
(b) G.J.P. Britovsek, V.C. Gibson, S.J. McTavish, G.A. Solan, A.J.P. White, D.J. Williams, B.S. Kimberley, P.J. Maddox, Chem. Commun. (1998) 849–850;
(c) B.L. Small, M. Brookhart, A.M.A. Bennett, J. Am. Chem. Soc. 120 (1998) 4049–4050;
(d) V.C. Gibson, C. Redshaw, G.A. Solan, Chem. Rev. 107 (2007) 1745–1776.
[4] W. Keim, F.H. Kowalt, R. Goddard, C. Kruger, Angew. Chem. Int. Ed. 17 (1978) 466–467.
[5] (a) N.A. Cooley, S.M. Green, D.F. Wass, K. Heslop, A.G. Orpen, P.G. Pringle, Organometallics 20 (2001) 4769–4771;
(b) J.N.L. Dennett, A.L. Gillon, K. Heslop, D.J. Hyett, J.S. Fleming, C.E. Lloyd-Jones, A.G. Orpen, P.G. Pringle, D.F. Wass, J.N. Scutt, R.H. Weatherhead, Organometallics 23 (2004) 6077–6079.
[6] (a) J. Heinicke, M.Z. He, A. Dal, H.F. Klein, O. Hetche, W. Keim, U. Florke, H.J. Haupt, Eur. J. Inorg. Chem. (2000) 431–440;
(b) J.M. Malinoski, M. Brookhart, Organometallics 22 (2003) 5324–5335;
(c) P. Kuhn, D. Sémeril, D. Matt, M.J. Chetcuti, P. Lutz, Dalton Trans. (2007) 515–528.
[7] (a) O. Daugulis, M. Brookhart, Organometallics 21 (2002) 5926–5934;
(b) F. Speiser, P. Braunstein, L. Saussine, R. Welter, Inorg. Chem. 43 (2004) 1649–1658.
[8] (a) C.M. Killian, L.K. Johnson, M. Brookhart, Organometallics 16 (1997) 2005–2007;
(b) E.V. Salo, Z. Guan, Organometallics 22 (2003) 5033–5046.
[9] (a) F. Speiser, P. Braunstein, L. Saussine, Inorg. Chem. 43 (2004) 4234–4240;
(b) T.R. Younkin, E.F. Connor, J.I. Henderson, S.K. Friedrich, R.H. Grubbs, D.A. Bansleben, Science 287 (2000) 460–462.
[10] P. Hao, S. Zhang, W.H. Sun, Q. Shi, S. Adewuyi, X. Lu, P. Li, Organometallics 26 (2007) 2439–2446.
[11] N. Ajellal, M.C.A. Kuhn, A.D.G. Boff, M. Horner, C.M. Thomas, J.F. Carpentier, O.L. Casagrande, Organometallics 25 (2006) 1213–1216.
[12] F.A. Kunrath, R.F.d. Souza, O.L. Casagrande, N.R. Brooks, V.G. Young, Organometallics 22 (2003) 4739–4743.
[13] Y.D.M. Champouret, J.-D. Marechal, W.R.K. Chaggar, J. Fawcett, K. Singh, F. Maserasc, G.A. Solan, New J. Chem. 31 (2007) 75–85.
[14] J. Hou, W.H. Sun, S. Zhang, H. Ma, Y. Deng, X. Lu, Organometallics 25 (2006) 236–244.
[15] L.L. de Oliveira, R.R. Campedelli, M.C.A. Kuhn, J.-F. Carpentier, O.L. Casagrande Jr., J. Mol. Catal. A: Chem. 288 (2008) 58–62.
[16] J.P. Sauvage, Acc. Chem. Res. 23 (1990) 319–327.
[17] (a) H. Tanaka, Y. Kin, M. Nakano, A. Usuki, Patent No. JP 2000344815, 2000342000;
(b) M.D. Doherty, S. Trudeau, P.S. White, J.P. Morken, M. Brookhart, Organometallics 26 (2007) 1261–1269.
[18] P. Yang, Y. Yang, C. Zhang, X.-J. Yang, H.-M. Hu, Y. Gao, B. Wu, Inorg. Chim. Acta (2008), DOI: 10.1016/j.ica.2008.1003.1018.
[19] G.J.P. Britovsek, S.P.D. Baugh, O. Hoarau, V.C. Gibson, D.F. Wass, A.J.P. White, D.J. Williams, Inorg. Chim. Acta 345 (2003) 279–291.
[20] (a) L. Wang, W.-H. Sun, L. Han, H. Yang, Y. Hu, X. Jin, J. Organomet. Chem. 658 (2002) 62–70;
(b) W.-H. Sun, S. Zhang, S. Jie, W. Zhang, Y. Li, H. Ma, J. Chen, K. Wedeking, R. Frohlich, J. Organomet. Chem. 691 (2006) 4196–4203.
[21] A.M.S. Garas, R.S. Vagg, J. Heterocycl. Chem. 37 (2000) 151–158.
[22] The Addison τ parameter 0.30 for 10b and 0.15 for 12b with τ = 0.0 for an ideal square pyramid and τ = 1.0 for an ideal trigonal bipyramid; see A.W. Addison, T.N. Rao, J. Reedijk, J. van Rijn, G.C. Verschoor, J. Chem. Soc., Dalton Trans. (1984) 1349–1356.
[23] C. Janiak, K.C.H. Lange, P. Marquardt, Macromol. Rapid Commun. 16 (1995) 643–650.
[24] F. Blank, C. Janiak, Coord. Chem. Rev. (2008), DOI: 10.1016/j.ccr.2008.1005.1010.
[25] G.J.P. Britovsek, S. Mastroianni, G.A. Solan, S.P.D. Baugh, C. Redshaw, V.C. Gibson, A.J.P. White, D.J. Williams, M.R.J. Elsegood, Chem. Eur. J. 6 (2000) 2221–2231.
[26] (a) C. Janiak, K.C.H. Lange, P. Marquardt, J. Mol. Catal. A: Chem. 180 (2002) 43–58;
(b) C. Janiak, in: A. Togni, R.L. Halterman (Eds.), Metallocenes, vol. 2, Wiley/VCH, Weinheim, 1998, p. 547, (Chapter 9);
(c) W. Kaminsky, R. Engehausen, K. Zoumis, W. Spaleck, J. Rohrmann, Makromol. Chem. 193 (1992) 1643;
(d) U. Stehling, J. Diebold, R. Kirsten, W. Röll, H.H. Brintzinger, S. Jüngling, R. Mülhaupt, F. Langhauser, Organometallics 13 (1994) 964;
(e) W. Spaleck, F. Küber, A. Winter, J. Rohrmann, B. Bachmann, M. Antberg, V. Dolle, E.F. Paulus, Organometallics 13 (1994) 954;
(f) N. Schneider, M.E. Huitenloch, U. Stehling, R. Kirsten, F. Schaper, H.H. Brintzinger, Organometallics 16 (1997) 3414.
[27] Q.Z. Yang, A. Kermagoret, M. Agostinho, O. Siri, P. Braunstein, Organometallics 25 (2006) 5518–5527.
[28] A. Kruis, In: H. Hausen (Ed.), Technik, Part 4, Vol. c, Springer, Berlin, 1976, p. 121.
[29] D.S. Breslow, C.R. Hauser, J. Am. Chem. Soc. 62 (1940) 2385–2388.
[30] C.F.H. Allen, R.D. Abell, J.B. Normington, Org. Synth. Coll. 1 (1941) 205.
[31] F. Barigelletti, B. Ventura, J.-P. Collin, R. Kayhanian, P. Gaviña, J.-P. Sauvage, Eur. J. Inorg. Chem. (2000) 113–119.
[32] G.M. Sheldrick, Program SADABS: Area-Detector Absorption Correction, University of Göttingen, Germany, 1996.
[33] G.M. Sheldrick, SHELXS-97, SHELXL-97, Programs for Crystal Structure Analysis, University of Göttingen, Germany, 1997.